ELSEVIER

Wavelength dependence of UV-laser induced emission of neutral and ionic species from single crystal NaNO$_3$

L.P. Cramer[a,*], S.C. Langford[a], W.P. Hess[b], J.T. Dickinson[a]

[a]Department of Physics and Materials Science, Washington State University, Pullman, WA 99164-2814, USA
[b]Pacific Northwest National Laboratory, P.O. Box 999, Richland, WA 99352, USA

Abstract

We report time-resolved, quadrupole mass-selected measurements of neutral and ion emission from single crystal sodium nitrate exposed to ns pulse excimer laser radiation at 157 nm (F$_2$ excimer, 7.9 eV photons), 193 nm (ArF excimer, 6.4 eV photons) and 248 nm (KrF excimer, 5.0 eV photons). Neutral emissions, including NO, O$_2$, N$_2$, and Na are observed at all three wavelengths. At 193 nm, intense atomic N and O emissions are also observed, possibly due to a 1 + 1 excitation involving the $\pi^* \leftarrow \pi$ transition in the nitrate ion (centered at 6 eV) followed by excitation to a higher excited state. This transition is not efficiently excited at the other two wavelengths. At 248 nm, much of the emission is attributed to thermally assisted, dissociative electron/hole attachment. Although 157 nm photons do not excite the $\pi^* \leftarrow \pi$ transition efficiently, the resulting NO emission is found to be quite intense: on a per unit energy (or per photon) basis, 157 nm photons are much more efficient in decomposing nitrate anions than 193 nm photons. Intense ion emission (principally Na$^+$ and NO$^+$) is observed at 193 and 157 nm, with weaker Na$^+$ emission at 248 nm. The ion intensities show high-order fluence dependence, consistent with photoelectronic emission involving sequential photon absorption as described earlier for 248 nm irradiation [J. Appl. Phys. (80) (1996) 6452]. © 2002 Elsevier Science B.V. All rights reserved.

Keywords: Sodium nitrate; Laser desorption; Ion emission; Photolysis

1. Introduction

Laser-induced particle emission from solid surfaces depends strongly on the laser wavelength and the details of bulk and defect absorption. Laser interactions in transparent, ionic solids are often much stronger in the ultraviolet, even at wavelengths well below the bandgap, usually due to absorption at defects. When the photon energy lies within a strong absorption band, emission mechanisms should be markedly altered. The question of how interaction strengths and emission mechanisms change as the laser wavelength is probed across a strong absorption band is largely unexplored in solid materials.

Although the bandgap of sodium nitrate exceeds 10 eV, it displays a strong absorption centered at 6 eV due to a $\pi^* \leftarrow \pi$ transition in the NO$_3^-$ anion. Irradiation at 213 and 193 nm (5.8 and 6.4 eV photons) at low laser fluences (energy per unit area) produce significant NO and atomic O emissions with thermal and hyperthermal components [2–5]. The neutral yields depend linearly on fluence, consistent with photoelectronic emission due to single photon absorption. In contrast, irradiation at 248 nm (5.0 eV photons—on the low energy edge of the $\pi^* \leftarrow \pi$ band) at higher fluences produces principally defect-related NO emission and negligible O emission; NO emission again

* Corresponding author. Tel.: +1-509-335-1698.
E-mail address: lpcramer@wsu.edu (L.P. Cramer).

depends linearly on fluence at fluences below 100 mJ/cm^2, also consistent with a photoelectronic emission mechanism [1,6–8]. The velocity distribution of the neutral fragments displays both fast and slow emission components. This emission is well accounted for on the basis of dissociative charge attachment at surface anion groups [1,6–10], where mobile electrons and/or holes are released from defect sites by single photon processes [1]. This is strongly supported by the observation that at 248 nm induction (incubation) is seen in the increasing NO emission intensity with number of laser pulses from $NaNO_3$ due to defect production [6] and the dramatic increase in NO (and O_2) emission intensity with exposure of the surface to electron beams (also generating defects).

Here, we explore emissions at 157 nm (F_2 excimer, 7.9 eV photons), at photon energies well above the peak of the $\pi^* \leftarrow \pi$ band, where the absorption cross-section is over an order of magnitude smaller than at 248 and 193 nm [11,12]. We find that neutral and ion emissions at 157 nm are quite intense despite the weak absorption (relative to 193 nm). The rate of anion decomposition at 157 nm is at least double the rate at 193 nm on per unit energy basis over the entire range of fluences employed. Nevertheless, intense atomic N and O emissions are observed at 193 nm that are absent at 157 nm, indicating that the emission (and probably absorption) mechanism changes as the wavelength is decreased from 193 to 157 nm.

2. Experiment

$NaNO_3$ single crystals were grown in our laboratory by slowly cooling $NaNO_3$ (99.0% pure, Alfa Aesar) from the melt. The resulting crystals were cleaved into 0.2 cm × 1 cm × 1 cm plates and mounted in vacuum on a 3D translation stage mounted directly in front of and normal to the axis of a UTI 100C quadrupole mass filter.

All experiments were performed in a vacuum chamber with base pressure $< 1 \times 10^{-9}$ Torr. Sample irradiation at 157 nm was performed with a Lambda Physik LPF 200 excimer laser (F_2) with a pulse width of 20 ns; the region between the laser and the vacuum system was flushed with dry N_2 to minimize transmission losses due to atmospheric water and O_2. Irradiation at 248 and 193 nm was performed with a Lambda

Physik LPX 205I excimer laser (KrF, ArF), with a pulse width of about 30 ns.

3. Results and discussion

3.1. Neutral time-of-flight signals

Depending on wavelength, the neutral products observed are NO, O_2 (not shown), Na (not shown), atomic N, and atomic O. Typical NO time-of-flight signals for each wavelength at a fluence of 85 mJ/cm^2 appear in Fig. 1. At this fluence, 157 nm irradiation yields by far the most intense NO signal, followed by 248 nm (17% of 157 nm) and 193 nm (6% of 157 nm).

The NO time-of-flight at 193 nm is noticeably faster than at the NO time-of-flight at the other wavelengths. A two-component thermal emission model provides a reasonable fit to the signal, with one component having a temperature near 1500 K and the other near room temperature. Knutsen and Orlando [4] interpreted a similar high temperature component under 193 nm excimer laser irradiation (≤ 1 mJ/cm^2) in terms of direct photoelectronic emission from the surface. In contrast, Bradley et al. found no high temperature component in similar measurements on a single rotational/vibrational state under 213 nm irradiation (5.8 eV photons, 5 ns pulses, <1 mJ/cm^2). A study of
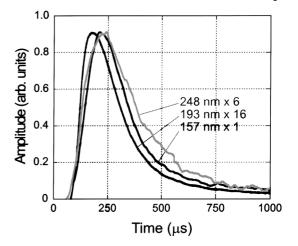
Neutral NO Emission from NaNO₃

Fig. 1. NO time-of-flight signals at 248, 193, and 157 nm at fluences of approximately 85 mJ/cm^2.

electron-stimulated desorption (ESD) of NO from $NaNO_3$ by Petrik et al. [13] indicate that the intensity and effective translational temperature depend strongly on rotational state, with some rotational states showing no hyperthermal component. In our work, the NO signals at 193 nm are consistent with NO production by single photon, photoelectronic decomposition of the anion; some molecules are emitted in a concerted fashion, yielding NO with a hyperthermal velocity distribution, while other molecules are desorbed after reaching thermal equilibrium with the surface.

The NO signals at 157 and 248 nm are slower. Nevertheless, the emission at 157 nm is still consistent with a two component model, with one fast component (equivalent temperature near 1500 K) and a slower component (temperature somewhat above room temperature). The fast component at 157 nm makes up a much smaller fraction of the total emission than the fast component at 193 nm.

The TOF signal at 248 nm is more complex, with a long tail on the low energy side of the peak. In previous work, we have shown that NO and O_2 emission at 248 nm persists for some hundreds of microseconds after the laser pulse. Delayed emission is also observed during pulsed electron irradiation [13,14]. As previously mentioned, emission of neutral anion fragments at 248 nm has been attributed to dissociative charge attachment (hole or electron attachment) [10,15]. Charge liberated during the laser pulse can remain mobile for some time after the laser pulse, resulting in dissociation events long after the laser pulse. This charge originates from defect states, which accounts for the linear fluence dependence (noted below) despite the low photon energy. The long emission tail at 248 nm appears to be unique among the three laser wavelengths employed in this work. Thus, delayed emission due to charge attachment appears to be far more important at 248 nm than at 193 or 157 nm. One possibility we are considering is that at the higher photon energies, electrons are more readily emitted into vacuum where they do not participate in anion decomposition. We plan to experimentally check the relative electron yields from $NaNO_3$ at these three wavelengths.

3.2. Neutral emission fluence dependence

The fluence dependence of the neutral NO, N, and O intensities at all three wavelengths appear in Fig. 2.
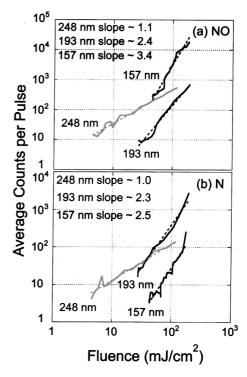

Fig. 2. Fluence dependence of (a) neutral NO and (b) neutral atomic N at 248, 193 and 157 nm.

Consistent with previous work [6], the NO intensity at 248 nm is an approximately linear function of fluence over this fluence range. In contrast, the fluence dependence of NO at 193 and 157 nm (6.4 and 7.9 eV) is non-linear (second to fourth order, at much lower fluences (<1 mJ/cm^2), Knutsen and Orlando [5] found a linear fluence dependence at 193 nm). The non-linear fluence dependence observed at the fluences employed here is not likely the result of non-resonant multiphoton absorption. More feasible is a *multiple photon* process involving sequential single photon absorption, similar to the mechanisms we have suggested for positive ion emission [16]. These multiple photon processes are normally dependent on the presence of defects. Defect driven processes are typically associated with the phenomenon of induction or incubation, where the intensity of a product measured at constant fluence increases under prolonged irradiation. We have observed such induction in the neutral NO signal from $NaNO_3$ at 248 nm, but have not yet performed the necessary experiments at 193 nm and 157 nm. The participating defects could be lattice

defects, such as vacancies, or electronic defects, such as excitons. For instance, exciton–exciton interactions can yield especially high energy (and thus possibly dissociative) excitations. Similarly, dissociative $1 + 1$ excitations involving long-lived intermediate states would depend non-linearly on fluence.

Fig. 2(b) shows the fluence dependence of the signal due to atomic N at the three wavelengths employed in this study. At 248 and 157 nm, this signal is quite weak and can be entirely attributed to fragmentation of NO and N_2 in the quadrupole ionizer; thus, at our level of sensitivity, we detect no atomic N from the sample at 248 and 157 nm. In contrast, the N signal at 193 nm is many times greater than the detected NO and N_2 signals, and thus accounts for the great majority of the total nitrogen (in all forms) emitted from the sample. Similarly strong atomic O signals (not shown) are also observed. At 193 nm, anion radiolysis is far more complete, yielding more atomic species, than radiolysis at 248 and 157 nm. We propose that this atomic emission is due to a $1 + 1$ excitation through the π^* state that produces an extremely unstable anion. The absence of significant atomic N emission at 157 nm is consistent with the expected absence of the $\pi^* \leftarrow \pi$ resonance at this wavelength.

We currently have no reasonable explanation for the higher yield of NO at 157 nm. The lack of likely resonance states suggests that the roughly third order fluence dependence observed for NO emission at 157 nm is not due to multi- or multiple photon absorption. We are exploring the role of defects in this emission as a possible explanation. We note that at the high end of the fluence range employed, 157 nm photons dissociate more than twice as many anions per unit incident energy (and nearly three times on a 'per photon' basis) than 193 nm photons. Given that laser absorption at 193 nm is at least an order of magnitude greater than at 157 nm, this is surprising and begs for an explanation.

3.3. Ion time-of-flight

Na^+ and NO^+ are observed at all three wavelengths, although significantly higher fluences are required to produce measurable NO^+ at 248 nm. Typical TOF signals for Na^+ and NO^+ are shown in Fig. 3 for all three wavelengths. At low fluences (<95 mJ/cm^2 at 193 and 248 nm and <70 mJ/cm^2 at 157 nm), the Na^+
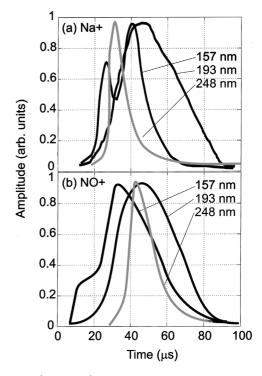

Fig. 3. Na^+ and NO^+ time-of-flight signals at 248, 193 and 157 nm, at fluences near 90 mJ/cm^2.

signals are adequately described by a single component, Gaussian energy distribution. The kinetic energy of this emission varies with wavelength and increases as the fluence is raised. At higher fluences, the Na^+ signal at each wavelength develops an additional peak at lower kinetic energies, which is well described by an additional Gaussian energy distribution. This slower peak displays kinetic energy distributions consistently in the 2–4 eV range. In previous work, we have observed both high and low energy Na^+ under 248 nm irradiation at fluences above 150 mJ/cm^2 [17]. Electrostatic arguments indicate that the photoionization of singly charged surface defects (e.g. surface vacancies with one trapped electron) would repel Na^+ adsorbed atop these sites with enough force to give them 2–4 eV of kinetic energy. The high energy ions (kinetic energies 7–10 eV) are attributed to emission from atop doubly charged defects, such as might be expected on modified surfaces with oxide-related surface defects [1,18,19].

In contrast, the NO^+ TOF signals cannot generally be described in terms of one or two well-behaved,
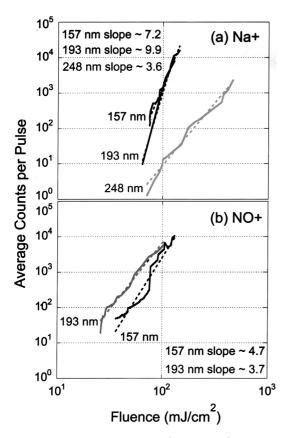
Fig. 4. Fluence dependence of: (a) Na^+ and (b) NO^+ emissions at 248, 193 and 157 nm.

Gaussian energy distributions. Both the TOF and energy distributions are quite broad and presumably represent emission from a wide variety of defect sites.

3.4. Ion fluence dependence

The Na^+ and NO^+ fluence dependence at 248, 193 and 157 nm are compared in Fig. 4. Na^+ emission in particular is strongly non-linear at 193 and 157 nm wavelengths (seventh to tenth order). It is highly unlikely that the photoionization of defect states would involve so many photons, even in a sequence of single-photon steps. As noted above, thermally activated processes can often mimic power-law multiple photon processes. The combination of ionization at several defects plus thermal activation would lead to this apparent high-order fluence dependence.

NO^+ emission at 193 nm is typically two orders of magnitude more intense than at 157 nm, suggesting that resonance absorption in the anion plays an important role in the emission process. This is true despite the fact that neutral NO emission is much more intense at 157 nm. In the absence of resonant ionization of gas phase neutral NO at both 193 and 157 nm (requires 9.24 eV), emission at one of these wavelengths (and probably both) must involve adsorbed NO^+ defects formed during anion decomposition or by hole trapping. Due to their initial association with the anion sublattice, these defects may experience a wide range of electrostatic environments, which would account for the wide range of observed kinetic energies.

4. Conclusions

Significant ion and neutral emissions are observed at each of the three excimer wavelengths employed in this study (248, 193, and 157 nm). Among the neutral species, NO and O_2 are emitted at all three wavelengths, while 193 nm radiation also yields intense atomic N and O emissions. We attribute the atomic N and O emissions to especially energetic dissociation events resulting from resonant (possibly sequential) two-photon excitation involving the $\pi^* \leftarrow \pi$ absorption centered at 6 eV. In contrast, N and O emissions at 157 nm are not detected, presumably due to the weakness of the $\pi^* \leftarrow \pi$ absorption at this wavelength. Despite this weak absorption into the π^* state, 157 nm photons decompose roughly twice as many NO_3^- anions per unit energy as 193 nm photons at the fluences employed in this work. This is a puzzling result that demands more study.

Significant Na^+ and NO^+ emissions are observed at 193 and 157 nm, with less intense emissions at 248 nm. The well-defined Na^+ kinetic energies argue for emission from equally well-defined defect states; the low kinetic energies are consistent with emission from sites atop singly charged anion vacancy defects. Most importantly, sample absorption at the laser wavelength does not completely control the strength of the laser interaction. An understanding of these effects will allow us to intelligently exploit the range of photon energies that are currently available in using lasers for processing,

surface modification, and chemical analysis of wide bandgap materials.

Acknowledgements

References

[1] D.R. Ermer, J.-J. Shin, S.C. Langford, K.W. Hipps, J.T. Dickinson, J. Appl. Phys. 80 (1996) 6452.

[2] R.A. Bradley, E. Lanzendorf, M.I. McCarthy, T.M. Orlando, W.P. Hess, J. Phys. Chem. 99 (1995) 11715.

[3] W.P. Hess, K.A.H. German, R.A. Bradley, M.I. McCarthy, Appl. Surf. Sci. 96-98 (1996) 321.

[4] K. Knutsen, T.M. Orlando, Phys. Rev. B 55 (1997) 13246.

[5] K. Knutsen, T.M. Orlando, Appl. Surf. Sci. 127-129 (1998) 1.

[6] R.L. Webb, S.C. Langford, J.T. Dickinson, Nucl. Instrum. Meth. Phys. Res. B 103 (1995) 297.

[7] J.T. Dickinson, J.-J. Shin, S.C. Langford, Appl. Surf. Sci. 96-98 (1996) 326.

[8] J.-J. Shin, M.-W. Kim, J.T. Dickinson, J. Appl. Phys. 80 (1996) 7065.

[9] J. Cunningham, J. Phys. Chem. 65 (1961) 628.

[10] J. Cunningham, in: E.T. Kaiser, L. Kevan (Eds.), Radical Ions, Interscience, New York, 1968, p. 475.

[11] H. Yamashita, R. Kato, J. Phys. Soc. Jpn. 29 (1970) 1557.

[12] H. Yamashita, J. Phys. Soc. Jpn. 33 (1972) 1407.

[13] N.G. Petrik, K. Knutsen, T.M. Orlando, J. Phys. Chem. B 104 (2000) 1563.

[14] J.-J. Shin, S.C. Langford, J.T. Dickinson, Y. Wu, Nucl. Instrum. Meth. Phys. Res. B 103 (1995) 284.

[15] J. Cunningham, J. Phys. Chem. 70 (1966) 30.

[16] J.T. Dickinson, in: J.C. Miller, R.F. Haglund (Eds.), Experimental Methods in Physical Sciences, Vol. 30, Academic Press, New York, 1998, p. 139.

[17] J.-J. Shin, D.R. Ermer, S.C. Langford, J.T. Dickinson, Appl. Phys. A 64 (1997) 7.

[18] J.T. Dickinson, S.C. Langford, J.J. Shin, D.L. Doering, Phys. Rev. Lett. 73 (1994) 2630.

[19] J.T. Dickinson, J.J. Shin, S.C. Langford, Appl. Surf. Sci. 96–98 (1996) 316.